X-ray diffuse scattering experiments from bismuth-based high-T_c superconductors

M. Izquierdo,[1,2] S. Megtert,[1] J. P. Albouy,[3] J. Avila,[1,4] M. A. Valbuena,[1,4] G. Gu,[5] J. S. Abell,[6] G. Yang,[6]
M. C. Asensio,[1,2,4] and R. Comes[1,3]

[1]*LURE, Centre Universitaire Paris-Sud, Bât.209D, B.P. 34, 91898 Orsay Cedex, France*
[2]*Synchrotron SOLEIL, L'Orme des Merisiers, Saint-Aubin, B.P. 48, 91192 Gif-sur-Yvette Cedex, France*
[3]*Laboratoire Physique des Solides, Centre Universitaire Paris-Sud, Bât. 510, 91405 Orsay Cedex, France*
[4]*Instituto de Ciencia de Materiales, CSIC, 28049 Madrid, Spain*
[5]*Physics Department, Building 510B, Brookhaven National Laboratory, Upton, New York 11975-5000, USA*
[6]*School of Metallurgy and Materials Science, University of Birmingham, Edgbaston, Birmingham, B15 2TT, United Kingdom*
(Received 28 February 2006; revised manuscript received 8 June 2006; published 29 August 2006)

A detailed study, by x-ray diffuse scattering, of the recently found two-dimensional (2D) displacive short-range-order (2DSRO) superstructure, with doubled periodicity along the orthorhombic $\mathbf{a}_o$ direction and perpendicular to the known long-range structural modulation, from the high-T_c superconductor $Bi_2Sr_2CaCu_2O_{8+\delta}$ (Bi-2212) is reported. The investigation has been extended to high and low temperatures for optimally doped crystals, to crystals with different doping levels, and to the one layer compound $Bi_2Sr_2CaCu_2O_{6+\delta}$ (Bi-2201). The results show that the 2DSRO is present at room temperature, for all studied crystals and with the same commensurate $2\mathbf{a}_o$ periodicity; significant differences in intensity and in the extent of the 2DSRO are however observed. The most striking feature is that both, the intensity of the diffuse scattering and the extent of the 2DSRO goes through a maximum for the optimal doped crystals and decreases for overdoped and underdoped samples, they are also smaller for the one layer Bi-2201 which has a lower T_c. The reversible temperature dependence reveals that the diffuse scattering is unchanged between 35 K and 300 K, but starts washing out for higher temperatures and vanishes around 450 K, temperature above which another scattering, one dimensional in character, is found. This one-dimensional (1D) short-range order (1DSRO) corresponds to linear correlated displacements along the pseudotetragonal directions of the Cu-O-Cu chains. These findings tend to show that these short-range ordering features may be of importance for a better understanding of high-T_c materials, at least those from the bismuth-based family.

I. INTRODUCTION

Investigations of the structural short-range order (SRO) properties of high-T_c superconductors have shown to be of great importance for the understanding of the physics that preside over their behavior. The driving force has been provided by a variety of theoretical work suggesting that SRO or structural correlations with different origin (magnetic or atomic) and character (static or dynamic) should exist in the high temperature superconductors.[1–8] In this respect, both local and extended probes have provided a wealth of data showing the existence of different types of SRO in different superconducting families (for a review see Ref. 8). Thus, neutron scattering has shown the existence of a charge and spin phase separation in "stripes" in two of the most most important families of compounds, namely $La_{2-x}Sr_xCuO_4$ (LSCO) and $YBa_2SrCu_3O_7$ (YBCO).[9–18] In the case of YBCO, although initially assumed rigid and oriented in one direction, recent experiments have pointed out that the nature of the spin excitations is two dimensional (2D) and more compatible with a liquid-crystalline stripe ordering.[19] Regarding the x-ray scattering investigations, the "relation" to "stripes" has been observed in Nd-doped LaSrCuO.[20] However, experiments on non-Nd-doped LSCO compounds have shown evidence of SRO with different origin: on the one hand, the existence of an incommensurate SRO rotated by 45° with respect to the magnetic pattern, therefore not related with "stripes," has been observed.[21] On the other hand, diffuse scattering ascribed to polaron formation has also been evidenced.[22] The investigations of the YBCO family have led to the observation of a complex phase diagram where different SRO phases develop as a function of doping and temperature starting from a high temperature tetragonal disordered phase.[23,24] In all the cases,[23–29] their origin is related with and ordering of the oxygen vacancies in the orthorhombic direction $\mathbf{a}_o$ perpendicular to the Cu-O chains running along $\mathbf{b}_o$. The different periodicity seems to depend on the oxygen doping, as predicted theoretically[24] and supported experimentally by the fact that the undoped compound $YBa_2Cu_4O_8$ does not exhibit diffuse features.[25] However, the picture seems to be more complex and for optimally doped samples (O stoichiometry 6.92) a four unit cell superstructure, expected near 6.75 stoichiometry, has been observed,[30] and attributed either to phase separation or non-negligible Coulomb interactions. Furthermore, in underdoped compounds the observed diffuse scattering has been interpreted as the presence of charged stripes whose periodicity uses that of the underlying oxygen ordering in the Cu-O chains due to an anomaly in the evolution of the intensity at the pseudogap opening.[28] However, this conclusion is not supported by other studies where this anomaly has not been observed.[25] On the contrary, results as a function of oxygen and trivalent atom substitution sustain a diffuse scattering depending on oxygen doping only, and not on the carrier concentration.[25] This idea is further supported by the fact that no signatures of charged stripes or charge density waves seem to be present in $YBa_2Cu_4O_8$, which does not have oxygen

vacancies.[25] In any case, it is worth mentioning that in spite of the controversy on some points, there seems to be a common agreement on the fact, that although the atoms are primarily displaced along the $\mathbf{a}_o$ axis, there exists an intensity modulation of the diffuse structures along $\mathbf{c}_o^*$, which means that the lattice displacements affect the whole unit cell.[23,25,28,30] On the other hand, experiments investigating the substitution of Cu by a trivalent metal have shown[26] that the host metal goes to the Cu-O chains and induces an oxygen ordering around them, thus leading to a local orthorhombic distortions with a coherence length important for the superconductivity.[26,27]

Regarding the bismuth-based superconducting cuprates, SRO has been extensively studied by means of STM,[8,31,32] which has revealed the existence at very low temperatures of a checkerboard pattern with 4 times periodicity along the tetragonal $\mathbf{a}_t$ direction. This observation has been interpreted either as a consequence of "stripe" ordering in these compounds or due to the scattering of quasiparticles. Away from the "stripe" models, it has been shown by both STM and theory that the oxygen dopants modify the electronic structure locally and therefore modulate the pair interaction.[33,34] Furthermore, some modulation suggesting a doubling of the unit cell along the orthorhombic $\mathbf{a}_o$ direction has been observed.[31,32] However, its extent is different in the two cases and the origin uncertain. On the other hand, extended probes studies using neutron diffraction have only shown a structure related with the magnetic resonance peak,[15] while x-ray diffuse scattering was not carried out at that stage. In this context, we have recently reported the existence of a new SRO or correlation in the Bi-2212 compounds by means of x-ray diffuse scattering experiments.[35] The short-range order consists in a doubling of the periodicity along the orthorhombic $\mathbf{a}_o$ direction, thus coexisting with and perpendicular to the well-known three-dimensional (3D) long-range-order structural modulation along $\mathbf{b}_o$. This local order is of displacive type and restricted to the $\mathbf{a}_o$-$\mathbf{b}_o$ planes parallel to the conducting layers (2D order).

In this paper, we present the results of an exhaustive investigation of the x-ray diffuse scattering on bismuth-based superconductors in order to provide a deeper understanding of the 2DSRO structure with doubled periodicity along the $\mathbf{a}_o$ direction recently reported.[35]

We have first concentrated on optimally doped crystals of both the Bi-2212 and Bi-2201 families and we have observed that for all studied samples (about a dozen crystals) the 2DSRO diffuse scattering at room temperature is always present. This strongly suggests that we are in the presence of a general feature in this family of compounds.

Second, a temperature dependence of the diffuse scattering for the optimally doped Bi-2212 samples has been carried out in the temperature range from 35 K up to about 650 K. The bare result is that two different types of scattering features are observed in the investigated temperature range. From 35 K up to about 300 K the observed diffuse scattering is temperature independent. A further increasing of the temperature above 300 K shows first a decrease of the 2DSRO related diffuse scattering intensity and an associated broadening of the diffuse features. Besides, a new type of diffuse scattering now revealing 1DSRO becomes observable

above about 450 K. This high temperature diffuse scattering corresponds to short-range order or correlations along the diagonal of the $\mathbf{a}_o$-$\mathbf{b}_o$ orthorhombic planar lattice, that is to say parallel to the axis of the pseudotetragonal lattice or the "Cu-O-Cu chains." On the other hand, the 3D long-range order structural modulation remains unaffected up to the highest temperature reached in the reported set of measurements.

Third and finally, a study of the evolution of the diffuse scattering features for the Bi-2212 compound has been carried out as a function of doping (between underdoped T_c =40 K and overdoped T_c=60 K). Starting from the optimal doped sample the 2DSRO diffuse features broaden both for underdoped and overdoped samples. More precisely, it is found that the associated domain size (or extent of the local order) corresponding to the diffuse scattering as a function of the doping level follows the same dependence as T_c. This provides a clear link between the observed diffuse scattering from the 2DSRO and superconductivity in these compounds.

The organization of the paper is the following: In Sec. II, the experimental conditions and the characteristics of the samples are given. In Sec. III, the room temperature results for the optimally doped Bi-2212 and Bi-2201 are shown. Section IV is devoted to the temperature dependence of the Bi-2212 optimally doped sample and Sec. V, to the doping dependence. Finally, in Sec. VI a discussion tries to elucidate both the origin of the diffuse scattering features and their importance related to the superconductivity in these compounds. The main conclusions of our research are summarized in Sec. VII.

II. EXPERIMENTAL CONDITIONS

X-ray diffuse scattering experiments in monochromatic transmission mode were performed with two different experimental setups in Orsay (France). The room and high temperature measurements were performed at beamline D43 of the DCI storage ring from LURE synchrotron. The Si(111) monochromator provided a photon flux in the order of 1.6 $\times 10^{10}$ photons/s/mm^2 for a current of 300 mA in the storage ring and a circular collimator of 800 μm diameter. The wavelength of the incoming photon was set to λ=1.45 Å in order to avoid the excitation of parasitic fluorescence from any of the heavy elements of the material (in particular copper). Diffractograms were recorded both using the so-called "fixed crystal-fixed film technique," which provides on the pattern a projection of a spherical cut of reciprocal space by the Ewald sphere, and the "precession" technique, which allows the recording of an undistorted image of a selected plane of reciprocal space. The measurements with these two configurations provide a large overview of reciprocal space and therefore are best suited when looking for unknown features that can exist outside of the regular Bragg reflections.[37] In both cases, the x-ray intensity was recorded on an image plate detector with a pixel size of 86×86 μm^2. An air flow type heating system allowed to cover the temperature range between room temperature and 650 K. The low temperature data were measured at the Laboratory of Solid State Physics (LPS Orsay). The x rays were obtained from an x-ray rotat-

TABLE I. Critical temperature, family, doping type, doping level, and labeling of the investigated samples. The (∗) in the two first Bi-2212 samples denotes the average doping level of these samples.

T_c	Family	Doping type	Doping level	Label
35	*2201*	Optimal doping	0.16	OD2201
40–57	*2212*	Underdoped	0.08*	U40-57K
50–60	*2212*	Underdoped	0.09*	U50-60K
60	*2212*	Underdoped	0.1	U60K
80	*2212*	Underdoped	0.12	U80K
92	*2212*	Optimal doping	0.16	OD2212
83	*2212*	Overdoped	0.18	O83K
77	*2212*	Overdoped	0.18	O77K
67	*2212*	Overdoped	0.2	O67K
60	*2212*	Overdoped	0.22	O60K

ing anode generator equipped with a double bent graphite monochromator ($\lambda = 1.54$ Å from copper K-α). Low temperature sample environment was provided by a closed cycle helium cryostat where temperature could be set within ±1 K. The x-ray intensity was recorded either by an image plate detector (room temperature and 35 K) or a 1D position sensitive detector to follow its temperature dependence.

The Bi-2212 and Bi-2201 single crystals were grown by the floating zone method and showed a sharp transition at their critical temperature T_c,[38,39] except for two samples in the underdoped region which exhibit a broad transition, one of them in the range from $T_c = 40$ K to $T_c = 57$ K and the other between $T_c = 50$ K and $T_c = 60$ K.[40] All investigated samples were obtained by peeling a thin layer from larger crystals with typical dimensions $2 \times 2 \times 0.01$ mm parallel to the corresponding orthorhombic axis $\mathbf{a}_o, \mathbf{b}_o, \mathbf{c}_o$ ($\mathbf{a}_o$-$\mathbf{b}_o$ being the "conducting plane"). The thickness of the samples was as close as possible to the optimal value $1/\mu_o\rho$, which for $\lambda = 1.45$ Å corresponds to $d = 11.5$ μm. In Table I we have summarized the properties of the different investigated samples, namely their critical temperature, their family and the type and doping level, the latter obtained from the T_c by applying the universal, empirically obtained relationship $T_c/T_{c,\max} = 1 - 82.6(p - 0.16)^2$.[41] In the last column we have included a label to identify each sample in the following text.

III. OPTIMALLY DOPED SAMPLES

Figure 1 shows the typical x-ray diffraction pattern obtained at room temperature and normal incidence geometry (the incoming photons and the $\mathbf{c}_o$ axis being parallel to each other) for two different optimally doped Bi-2201 samples, panels (a) and (b), and one for the Bi-2212 compound, panel (c). In the case of Fig. 1(a), the sample to image plate distance was kept to $d = 50$ mm while for the other two a value of 75 mm was chosen, thus reducing the sampled portion of the reciprocal space. The white lines depicted in the diffractograms represent the iso-h lines resulting from the intersection of the reciprocal planes with $h = $ constant of the average
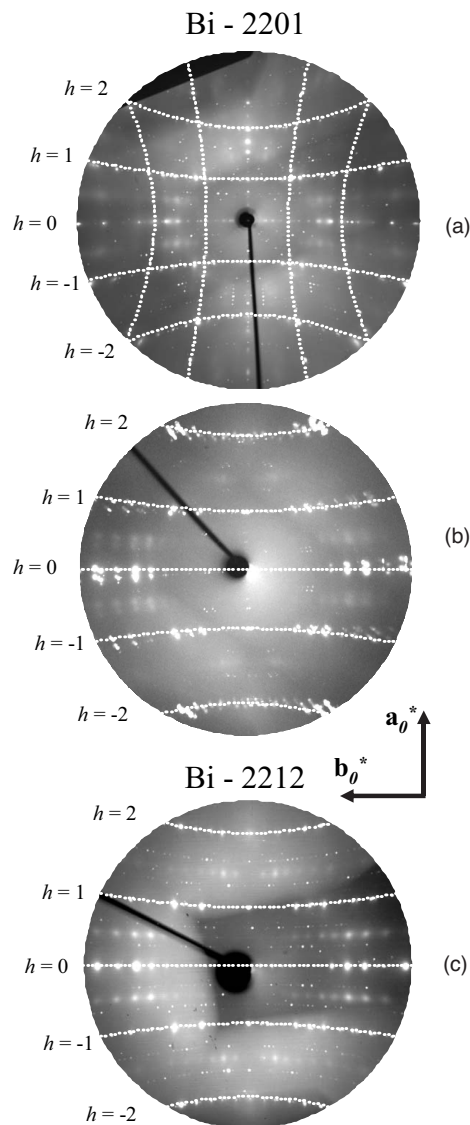

FIG. 1. X-ray diffuse scattering pattern of two Bi-2201 crystals measured with the fixed film-fixed crystal technique. The incident x-ray beam ($\lambda = 1.45$ Å) and the $\mathbf{c}_o^*$ axis are parallel to each other. Traces of reciprocal planes with h index constant are indicated as dotted lines. The two types of Bi-2201 samples (a) and (b) differ by the relative orientation of the different domains. In panel (c) a typical diffractogram for the optimally doped Bi-2212 compound is displayed for comparison.

structure and the Ewald's sphere. Concentrating on the data, we can see that the most striking difference between the three diffractograms arises from the fact that while for the Bi-2212 compound the samples have only one domain, all the Bi-2201 investigated samples exhibit always more than one. In particular, in Fig. 1(a) two domains rotated by 90° can be seen and three domains in Fig. 1(b) with a small misorientation angle between them are present. The former situation was the most commonly observed and can be understood by considering the natural tendency of these compounds to be twinned in the $\mathbf{a}_o$-$\mathbf{b}_o$ directions.[39,42,43] The small misoriented domains would correspond to regions
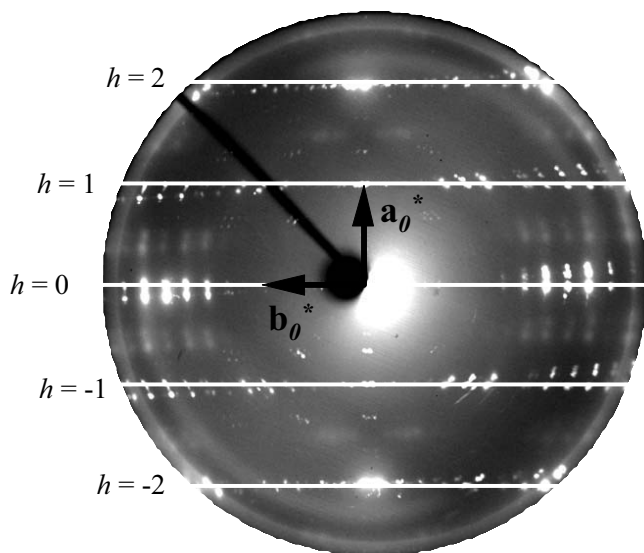
FIG. 2. Precession diffractogram for a Bi-2201 crystal with slightly misoriented domains. Solid lines represent the reciprocal planes with *h* index constant.
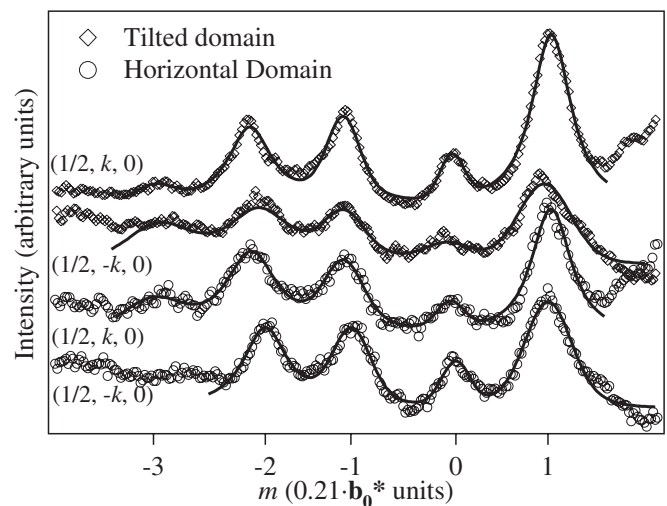

FIG. 3. Profiles along the $\mathbf{b}_o^*$ direction taken from the precession diffractogram of the Bi-2201 sample. Data after background substraction are displayed as open circles and diamonds for the horizontal and most intense tilted domains, respectively. The best obtained fits are plotted as solid lines.

separated by low angle grain boundaries and can even be visible under a polarized microscope.[39] To interpret the origin of the different diffuse features present in the diffractograms let us concentrate on the Bi-2212 sample [Fig. 1(c)]. We can clearly see the layers ($h=0,\pm1,\pm2$) where sharp Bragg reflections from the average structure are found together with satellites reflections from the long-range superstructure modulation $\mathbf{q}_b=0.21$ along the $\mathbf{b}_o^*$ direction. Besides them, we can also see very tiny spots corresponding to $\lambda/3$ contamination. Finally, there are broad diffuse scattering spots, which are clearly visible on the layers $h=\pm1/2,\pm3/2,\pm5/2$, they correspond to the recently observed $2\mathbf{a}_o$ diffuse scattering.[35] When going back to the Bi-2201 diffractograms we can observe in both cases the same different types of spots, although in this case with the multidomain structure characteristic of each sample. The presence of diffuse spots similar to those previously observed with Bi-2212 is particularly remarkable[35] showing that we are dealing with a general property of the bismuth based superconductors.

To assess the similarity of the diffuse features in the two families of compounds we must corroborate whether, besides the periodicity, the other properties of the diffuse scattering structure are similar, namely the dimensionality, the origin and the domain size. Fixed-crystal measurements performed in nonperpendicular configuration (not shown) confirm that the diffuse scattering consists of streaks parallel to the reciprocal $\mathbf{c}_o$ axis and characteristic of 2DSRO. To estimate the size or the extent of the local order and to unravel whether it arises from atomic displacements or chemical substitution we have performed precession measurements which provide an undistorted image of a selected reciprocal space plane. Figure 2 shows such a pattern obtained for the $(h,k,0)$ plane of the Bi-2201 sample with three slightly misoriented domains with solid iso-*h* lines corresponding to the intersection of the Ewald's sphere with reciprocal *h*=constant planes for

the biggest crystallite. We have oriented the diffractogram with the orthorhombic $\mathbf{a}_o$ and $\mathbf{b}_o$ axes parallel to the most intense crystallite and afterwards estimated the misorientation angle for the other two, which resulted to be 3.3° for the second most intense one and around 5° for the weakest. Regarding the Bragg reflections, we can clearly observe those of the long-range superstructure modulation, with a wave vector of 0.2 along the $\mathbf{b}_o^*$ axis, as generally reported. The presence of weak $\lambda/2$ contamination can account for the presence of the forbidden reflections $(1,0,0)$, $(-1,0,0)$, $(0,1,0)$, $(0,-1,0)$. Regarding the diffuse spots, we can see that their position follows that of the long-range superstructure modulation.

The quantitative estimation of the position of the diffuse spots is in agreement with our expected value $0.5\mathbf{a}_o^*$ found for Bi-2212. The analysis of the diffuse profiles measured along the $\mathbf{b}_o^*$ direction is shown in Fig. 3. In this case, four profiles were taken, two along the $\mathbf{b}_o^*$ of the horizontal domain and the other two for the second most intense tilted one. The results show that the positions of the diffuse spots are concurrent with those of the long-range superstructure modulation. The linewidths provide an average value of $(0.109\pm0.025)\mathbf{a}_o^*$ and $(0.119\pm0.04)\mathbf{a}_o^*$ for the horizontal and tilted domains, respectively. These values correspond to an average domain size of about 48 Å, which is somewhat smaller than the 60 Å value obtained for the Bi-2212 optimally doped crystals.[35]

IV. TEMPERATURE DEPENDENCE

In this section we will concentrate on the temperature dependence of the diffuse scattering from the Bi-2212 optimally doped crystals. Figure 4 displays two patterns at low temperatures, 297 K and 37 K, obtained with a conventional x-ray source as described in Sec. II. Figure 5 illustrates two
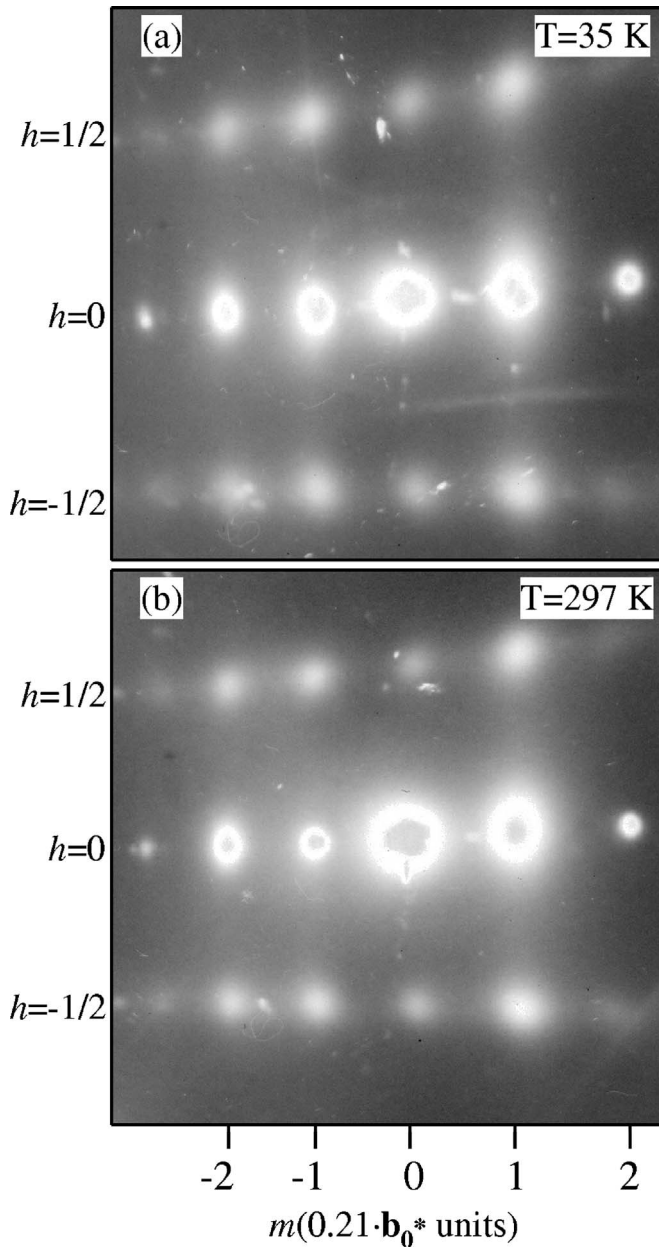
FIG. 4. Experimental x-ray diffractograms measured in the low temperature regime: (a) at $T=35$ K and (b) at room temperature. In both cases we clearly see the diffuse structures characteristic of the 2DSRO with the same intensity (see text for details).
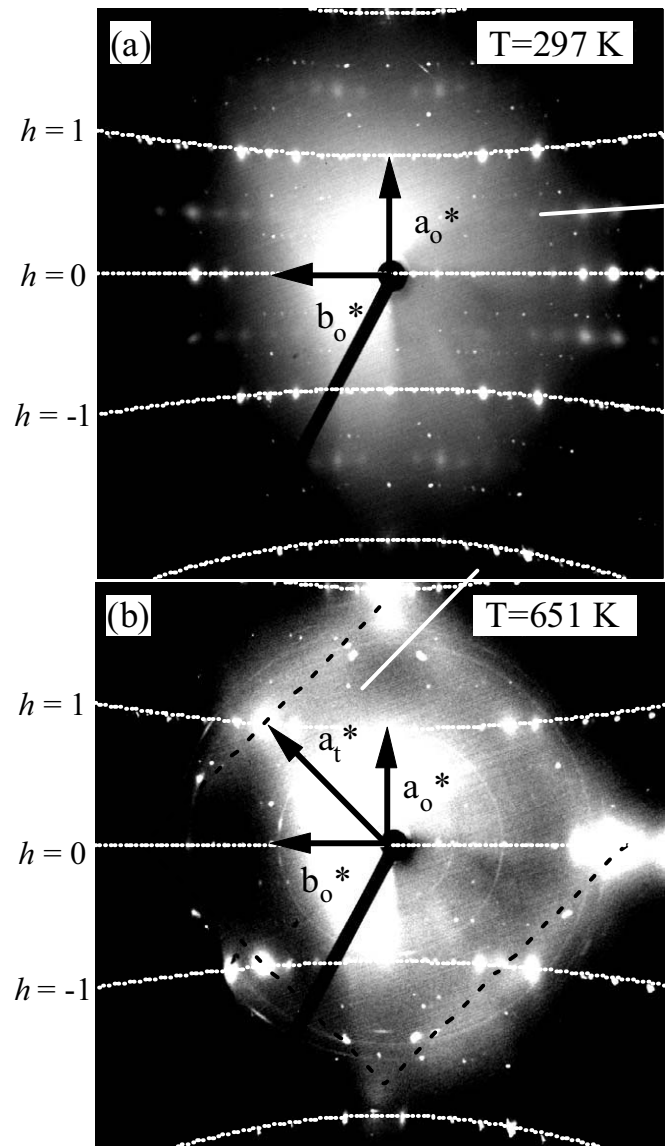

FIG. 5. Experimental x-ray diffractograms of the optimally doped Bi-2212 samples measured in the two different temperature regimes: (a) at room temperature, showing the presence of the $2\mathbf{a}_o$ diffuse structure, and (b) at $T=651$ K where only the 1D structure can be appreciated (indicated as dashed black lines). The solid white lines in both figures correspond to the profiles taken for the quantitative analysis.

typical diffractograms, respectively, at room temperature and at the highest investigated temperature of 651 K as obtained with x-ray synchrotron radiation. In both cases, the crystal orientation is such that the stacking $\mathbf{c}_o$ axis is parallel to the incident x-ray beam and perpendicular to the flat film or image plate surface (with some offset for the patterns of Fig. 4). In Fig. 5, superimposed on the diffractograms iso-index lines according to the orthorhombic reciprocal lattice $1/\mathbf{a}_o$ are shown $(\mathbf{a}_o \sim 5.4$ Å).[36] The well-known 3D long-range-order modulation is clearly seen on all patterns along the different iso-h lines as tiny and intense diffraction spots (the $\mathbf{q}_b$ wave vector component value is $0.21\mathbf{b}_o^*$).

On the room temperature patterns, which are also representative of the low temperature range, one can see the broad diffuse scattering features halfway between zero and first h levels, and above $h=1$, as already described above in Sec. III. The observation of this diffuse scattering holds from 35 K up to about 450 K although the diffuse spots broaden and the related intensity decreases for temperatures above 300 K and vanishes at about 450 K. At still higher temperature [Fig. 5(b)], another broad diffuse scattering of very low intensity becomes visible in the form of diffuse lines at about 45° from the main orthorhombic layers of the patterns. Owing to our fixed geometry these lines originate from diffuse intensity located in planes perpendicular to the reciprocal

direction $(h, k = \pm h, 0)$. This is the signature of a 1D local order or correlated movements of atoms in real space parallel to, or along the "CuO chains," that is to say along the in-plane axis equivalent to the pseudotetragonal unit cell. The location of the diffuse lines corresponds to a periodicity precisely equal to $\mathbf{a}_t^* = 1/\mathbf{a}_t$. The intensity distribution along the diffuse lines does not seem to vary or at most very smoothly indicating no or little correlations between parallel chains as expected from 1DSRO. We have performed several temperature cycles and observed these phenomena systematically and reversibly for all samples.

The quantitative characterization (intensity and linewidth) of both, the 2D and the 1D diffuse features, has been performed by monitoring the temperature dependence along the solid straight white lines shown in Figs. 5(a) and 5(b). In Fig. 6 we have used the orthorhombic description for the 2DSRO case and the notation (h, k, l, m) for the localization of any diffraction peak, where the index m stands for the order of the satellite peak with respect to the nearest main Bragg reflection and for the 1DSRO the simpler pseudotetragonal lattice reference. Figure 6(a) presents examples of the intensity profiles after background substraction of the diffuse scattering spots $(1/2, k, l, m)$ lying on the iso-h level with $h = 1/2$ in the temperature range between room temperature (RT) and 463 K. The circles correspond to the experimental data after background substraction and the solid lines to the best fitting obtained with five Voigt functions. Regarding the high temperature 1DSRO, a series of intensity profiles perpendicular to the diffuse lines (parallel to the reciprocal $\mathbf{a}_t^*$ tetragonal direction) are shown in Fig. 6(c). The profiles shown in Fig. 6 and the low temperature data mentioned previously provide both the average extent of the local order or domain size (inverse linewidth) [Fig. 7(a)] and the integrated intensity [Fig. 7(b)] as a function of temperature. The extent or domain size corresponding to the the 2DSRO remains constant from 37 K up to room temperature and from there it decreases almost linearly until it disappears around 450 K, the integrated intensity follows the same tendency as the domain size. The behavior of the 1DSRO is completely different, the average extent of the local order or chain length remains constant and only an increase in intensity is observable with increasing temperature. Some consequences of these observations will be discussed in Sec. VI.

V. DOPING DEPENDENCE

In this section, we will concentrate on the characterization of the 2DSRO as function of doping performed for the Bi-2212 at room temperature. This study is of crucial importance since it will allow us to elucidate whether this structure is related with the superconductivity of these compounds. In Fig. 8 we have displayed three enlarged portions from the precession patterns of the $(h, k, 0)$ reciprocal space plane around the $(0\,2\,0)$ diffraction peak from three samples, which cover the different doping regimes: underdoped 80 K (U80K), optimal doping (OD) and overdoped 83 K (O83K). Besides the normal Bragg peaks from the average structure $(0\,2\,0\,0)$ and from the satellites $0.21\mathbf{b}_0^*$ superstructure modulation $(0\,2\,0\,m \neq 0)$, we observe the presence of diffuse spots
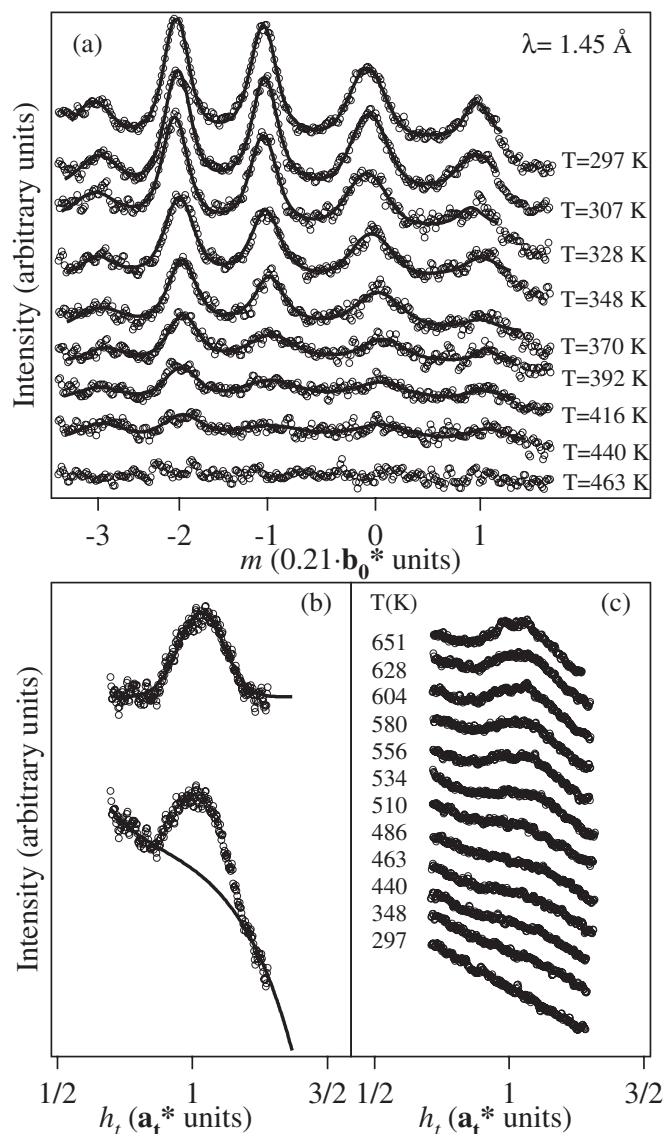

FIG. 6. (a) Profiles of the diffuse structure taken along the $(1/2\,k\,l\,m)$ line measured in the temperature range between 297 and 463 K together with the solid line obtained for the best fit (solid lines). (b) Example of 1D diffuse structure at 651 K: raw data and extracted profile. (c) Raw profiles as a function of the temperature for the 1D diffuse structure taken along the white line in Fig. 5(b).

as presented above for the 2DSRO. The differences of the diffuse intensities between the different patterns shown can be attributed to the variable thickness of the samples but we can see that they appear always at the commensurate $2\mathbf{a}_o$ value, irrespective of doping. Even qualitatively we can observe that the 2DSRO diffuse spots are most clearly visible at optimal doping and become much broader upon entering both the underdoped and overdoped regimes.

In Fig. 9 we display the intensity profiles versus reciprocal space position obtained for all the measured samples. From the profiles taken along the $(h\,2\,0\,1)$ line ($\mathbf{a}_o^*$ direction) displayed in Fig. 9(a) it is confirmed that the periodicity of the 2DSRO stays commensurate to the $2\mathbf{a}_o$ value in the whole doping range. The profiles along the $\mathbf{b}_o^*$ direction, displayed in Fig. 9(b), were taken along the $(1/2\,2\,0\,m)$, which
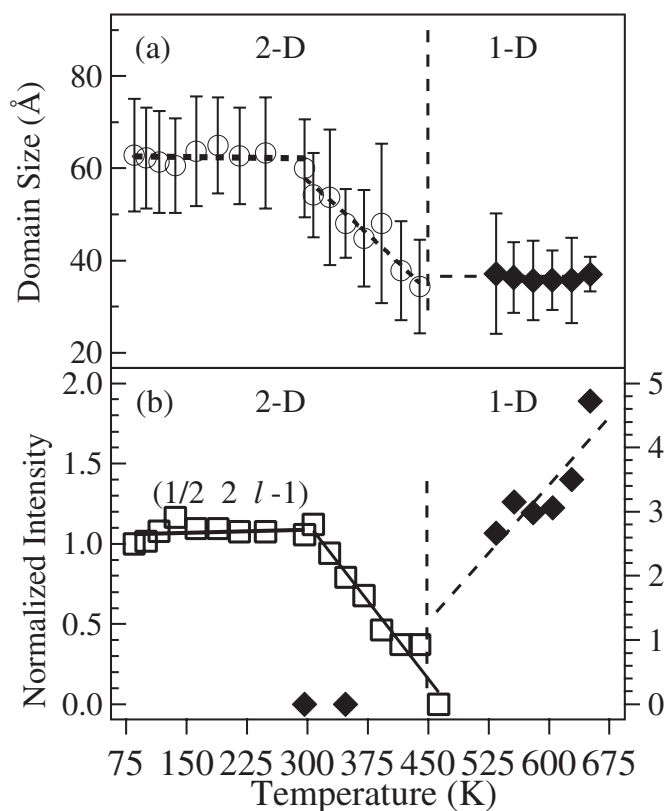
FIG. 7. (a) Domain size and chain length obtained from the linewidth of the diffuse 2D and 1D diffuse structures. (b) Integrated intensity as a function of temperature. The lines have been drawn as a guide to the eye.

is representative of the different $h=\pm1/2$ directions. The data are displayed as circles together with the best fit obtained with four Voigt functions (solid lines). We can notice that the profiles for all the different samples have the same properties: they follow the $0.21\mathbf{b}_o^*$ superstructure modulation, the $(1/2\ 2\ 0\ 0)$ spot has smaller intensity than its neighboring spots and the intensity increases upon increasing the supermodulation index m, that is when we get further away from the reciprocal space center. Regarding the intensity, even qualitatively, we see that it seems to reach a maximum at optimal doping and decreases upon entering in the overdoped and the underdoped regime. The drop in intensity is quite drastic as we move away from the optimally doped region and somewhat stronger in the overdoped region, where the diffuse spots can be hardly detected for samples with T_c lower than 83 K measured in the precession mode. This decrease is less pronounced for the underdoped samples, which can be accounted by (i) the crystal quality of the available samples gets poorer with underdoping (optical observation) and the onset of the superconducting transition from the studied samples, broader (conductivity); (ii) very low doping level crystals were not obtained and could not be studied. One of the underdoped crystals revealed different profiles of the diffuse spots according to the areas hit by the incoming x-ray beam (U40-57K) suggesting the presence of grains with different transition temperatures.

From the fitting of the profiles displayed in Fig. 9(b) we have quantified the domain size of the 2DSRO for the differ-

ent samples. For its estimation we have considered all the spots seen in Fig. 9(b) but $m=-2$, which could hardly be observed for the very overdoped samples. The results are displayed in Fig. 10, together with the values obtained for the two underdoped samples with a broad superconducting transition (U40-57K and U50-60K), which we have only measured in "fixed mode" due to the low intensity of the diffuse features. We observe that both the linewidth and the intensity (not shown) exhibit a parabolic behavior with a relative maximum at optimal doping. It is worth mentioning that the sample with the lowest T_c (U40-57K) the 2DSRO showed two different sizes and intensities, thus confirming the presence of two grains with different transition temperatures. Therefore, we could assume that the upper point for this doping level corresponds to the higher T_c and therefore it should be placed at higher doping levels in Fig. 10, thus enhancing the quality of the parabolic fitting. In any case, we can safely draw the conclusion that the behavior of the 2DSRO is similar to the scaling of the superconducting transition temperature T_c with doping, which establishes a clear link between the superconductivity and the observed 2DSRO diffuse features in these compounds.

VI. DISCUSSION

Before trying to get an overall physical picture taking into account all these observations it is useful to summarize the basic analysis which can be made of the reported diffuse scattering experiments. In all patterns it is easily noticed that the intensity of the diffuse scattering, on average, increases for an increasing scattering angle or, in other words, when going away from the incident beam. This is characteristic of displacive short-range order whether static or dynamic (i.e., phonons). In the case of a chemical short range order on the contrary, it would decrease sharply for increasing scattering angle as does a x-ray scattering factor (or a linear combination in presence of several displaced atoms) and this can be easily discarded here. Thus the observed diffuse scattering originates from correlated atomic displacements away from their average position (including the long-range structural modulation). The diffuse scattering is exceptionally intense and of the order of 0.1% of a regular nearby Bragg peak; this points either to large displacements, to a heavy atom, such as bismuth here, or both, which appears natural considering that the doping oxygen accommodates in the Bi-O planes.[45] In a simple structure the square root of the ratio of the diffuse intensity to a neighboring Bragg peak gives an order of magnitude of the displacement relative to the lattice constant (here 3.3%). In the case of multiatomic structures, the measurement of a number of diffuse scattering spots allows in principle to derive a set of atomic displacements (or phonon modes); here, given not only the complex structure but also the additional existence of the long-range modulation, it is almost impossible. The conclusion is that the main source of the diffuse scattering reported arises from displaced Bi atoms, but other atoms can also be associated.

In order to go further, we can first consider the temperature dependence of the diffuse scattering from the optimally doped samples and the question of a possible relation be-
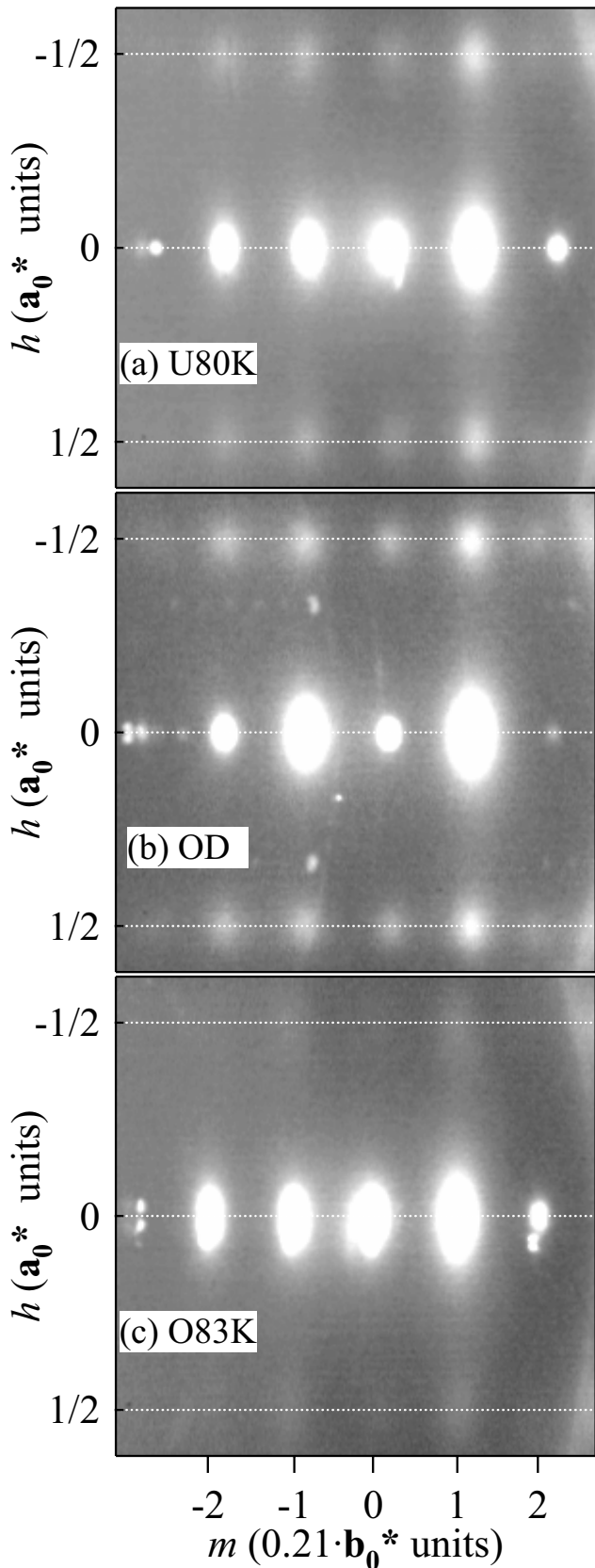
FIG. 8. Detail of the precession diffractogram measured for three of the Bi-2212 samples: (a) underdoped 80 K (U80K). (b) Optimal doping (OD) and (c) overdoped 83 K (O83K). We observe the presence of diffuse spots at the $h = \pm 1/2$ positions.
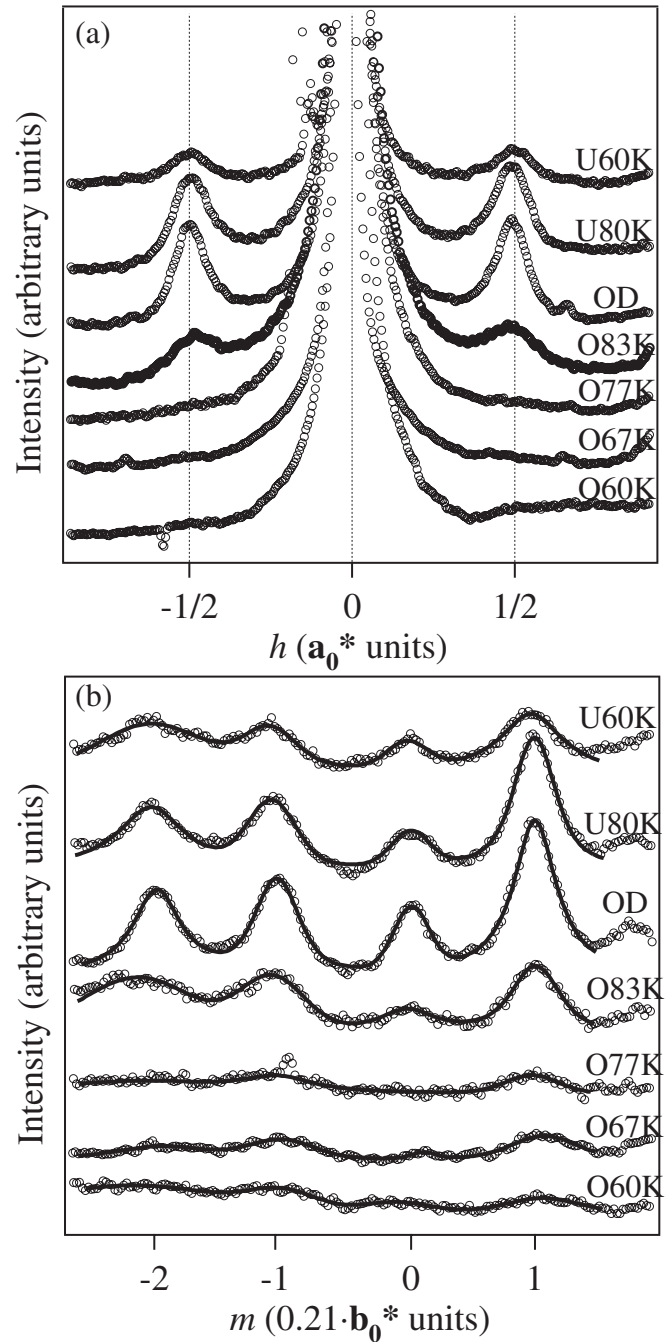

FIG. 9. (a) Profiles of the diffuse structure taken along the $(h\,2\,0\,1)$ line ($\mathbf{a}_o$ direction) and along the $(1/2\,k\,0\,m)$ ($\mathbf{b}_0$ direction) as a function of doping. Circles represent the data after background substraction and the solid lines in (b) the results of the best fit obtained with a four Voigt function.

tween the 2DSRO and the 1DSRO observed above 450 K. It is indeed tempting to think of two different regimes of the same phenomenon: high temperature 1D correlations or short-range order along chains oriented along the Bi-O-Bi and/or Cu-O-Cu chains coupling in the layer planes when the temperature is lowered so as to generate the 2DSRO which is then stabilized for temperatures below room temperature. Indeed, this idea would also explain the fact that both diffuse structures coexist with the 0.21 superstructure modulation by
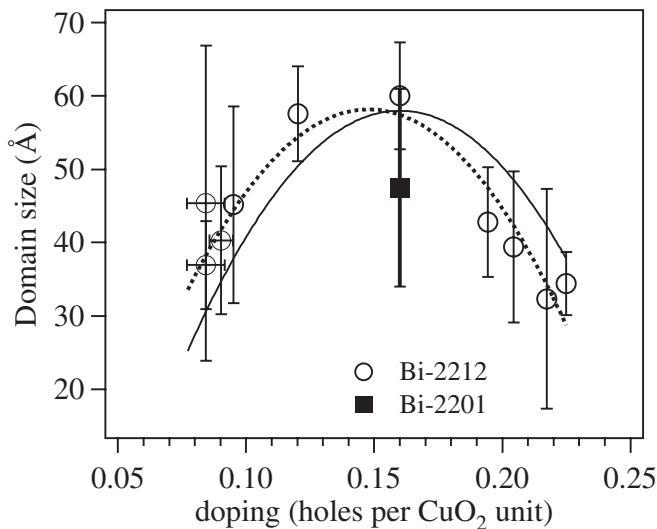
FIG. 10. Domain size from the analysis of the linewidth of the diffuse spots displayed in Fig. 2(b). The dashed line represent the best fit obtained for the data and the solid one the empirical parabola of the T_c vs doping (see text for details).

FIG. 11. (Color online) Allowed displacive modes obtained from the symmetry analysis.

considering that they appear by the freezing of the atomic displacements upon lowering the temperature starting from an initial supermodulated phase in a similar way as the different phases develop in YBCO from the high temperature tetragonal phase.[23] With this assumption a qualitative model of the atomic displacements can be obtained from an analysis of the symmetry of the displacement modes which could be concerned with this local order. Such analysis shows that there are only two one-dimensional (1D) irreducible representations of the small group associated with the star **q** $=1/2\,\mathbf{a}_o^*+q_b\,\mathbf{b}_o^*+0$ (or 1) $\mathbf{c}_o^*$, starting from the high symmetry *Bbmb* space group. From these ones, depicted in Fig. 11, one can deduce the atomics displacements compatible with the crystal symmetry. In principle, these displacements could take place either in the Bi$_2$O planes, in the Cu$_2$O layers or both. However, the latter is not likely to be happening here since the behavior of the diffuse spots is the same in the one and two layer compounds and there seems to be no scaling as a function of the number of layers. This contrasts with the fact that while in the Bi-2212 compounds the Cu and Bi atoms have the same symmetry chart, in the case of Bi-2201 this is not the case and therefore one would expect a different behavior between the two compounds if both the Cu and Bi atoms were involved. Considering more closely the displacement patterns of Fig. 11, which are shown relative to the orthogonal lattice axis, it may be worth noting that along the pseudotetragonal axis at 45°, the periodicity happens to quadruple the tetragonal lattice constant as observed by STM measurements at very low temperatures.[8]

There are however several objections to this common approach correlating the two diffuse scattering features. The most important one comes from the temperature dependence of both (i) the integrated intensity and (ii) the width of the diffuse scattering. If we concentrate on the 2DSRO features we can observe that both the domain size and the integrated intensity behave the same way with respect to temperature:
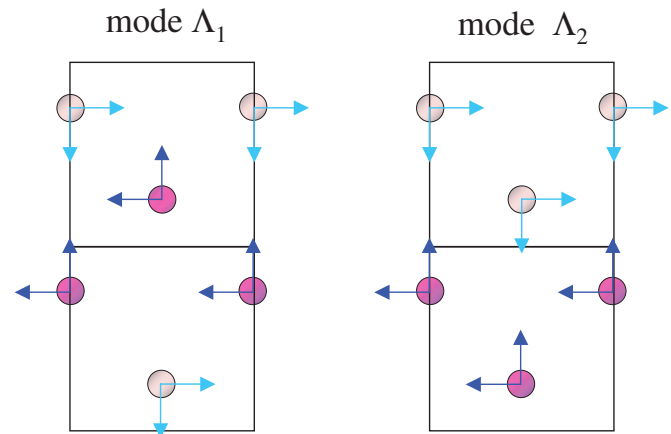
they are more or less constant from the superconducting state up to about RT, from where they decrease following an almost linear behavior until they vanish at about 467 K. On the contrary, for the high temperature 1DSRO above 450 K the width of the diffuse scattering remains constant while its intensity increases steadily. This contrasted behavior is not consistent with the image of a common origin where the increasing length of linear correlations (1DSRO) triggers a 2D coupling in the layers leading to a 2DSRO when the temperature is lowered. Moreover, one can note that the constancy of the intensity of the diffuse scattering of the reported 2$\mathbf{a}_o$ modulated superlattice over a large temperature range raises questions about some phonon assisted mechanism[21] and does not follow the behavior expected for conventional "stripes" either.[10,11]

Alternatively, one can consider the 1DSRO and the 2DSRO as unrelated features. In this framework, for the high temperature 1DSRO, a possible interpretation in terms of 1D ferroelectric fluctuations similar to those earlier observed in many perovskites (BaTiO,[3] KNbO,[3] KTaO,[3] etc.[44]) both by x-ray and neutron scattering would be consistent with the experimental observation. The increasing intensity with increasing temperature simply reflects the increasing amplitude of the corresponding phonons from a dispersion spectrum with planar valleys perpendicular to the pseudotetragonal axis; given the low intensity of the corresponding diffuse scattering it is tempting to think of fluctuations along the Cu-O-Cu axis where in successive Cu-O pairs the copper and oxygen move toward each other. For the 2DSRO the behavior of the diffuse scattering as a function of increasing temperature above RT with its loss in intensity, its broadening and the reversibility with respect to temperature cycles recalls *order-disorder* scenarios as usually observed in alloys, or heavily doped other materials. So far, and because of its relatively strong intensity, the corresponding diffuse scattering was mainly attributed to displacements of bismuth atoms (other atoms are not excluded, but with copper displacements of equal magnitude the x-ray signal would be almost one order of magnitude smaller), but such displacements could be triggered by a short-range order of doping oxygen in the BiO$_2$ layers which would also account for its quasi-2D na-

ture. Displacements of bismuth atoms triggered by ordered doping oxygen was indeed already strongly considered from structural data by Le Page.[45] In such a context, starting from the higher temperatures, mobile disordered doping oxygen (or a part of them) could progressively become short-range order when the temperature is lowered until a certain stable size depending on the doping level is reached and does not show further changes, as shown from the experimental results described above. Another possible interpretation for the 2DSRO, which would relate it with the long-range ordered incommensurate modulation, would be to consider that the long-range modulation very likely implies domains where the atomic displacement pattern is in opposition to the phase. At the boundaries between such domains one can imagine limited areas where the phase of the long-range modulation along the orthorhombic $\mathbf{b}_o$ axis simply alternates in parallel successive chains and in this way doubles locally the periodicity in the orthorhombic direction. Such "antiphase" effects could explain the existence of the 2DSRO. However, in this case, a link between the two diffuse structures would have to be again recalled, since the long-range ordered superstructure modulations remain at the higher temperatures, where the 2DSRO is no longer present but the 1DSRO is.

Concentrating on 2DSRO, one can say that its observation in the Bi-2201 samples indicates that we are dealing with a general feature of this family of compounds. Furthermore, the behavior of the 2DSRO as a function of doping for the Bi-2212 compounds shows that the $2\mathbf{a}_o$ periodicity remains commensurate and constant as a function of doping. These observations, together with the fact that the 2DSRO is observed at room temperature and the reported temperature dependence of the integrated intensity, does not support scenarios based on conventional "stripe" models.[9–18] When relating them with the "bubble phase" theoretically proposed by Spivak and Kivelson,[46] some similarities are observed, although as in the case of conventional stripes this phase only exists in a limited temperature range, which is not the case here. However, the SRO could be compatible with other types of inhomogeneous structures recently proposed for these cuprates.[47] When looking at the behavior of the domain size with doping (Fig. 10) we can observe that the domain size scales with the doping level following the same law as the one empirically obtained for the T_c.[41] This result is extremely important because it indicates that the observed SRO structure is related with the superconductivity of these compounds. On the other hand, when comparing with the Bi-2201 samples at optimal doping we observe that the ratio between the domain sizes is *Domain*(Bi-2212,OD)/*Domain* (Bi-2201,OD)=1.26. This ratio does not scale with the ratio between the maximal critical temperatures, as observed for other parameters like the superconducting gap or the pseudogap.[6] Actually, one can notice that the domain size for the optimally doped Bi-2201 compound is comparable to that of the U60K sample in the underdoped side and slightly higher than that of the O83K sample. This suggests that the diffuse scattering is more related to the excess oxygen than to the value of the critical temperature (otherwise the value would me much lower for the Bi-2201 samples) and therefore a similar parabolic behavior, with the maximum value being 45 Å is expected for this family of compounds. Since

the dopant oxygen goes into the Bi-O planes[45] we expect, in consequence, that the intensity modulation comes mainly from these atoms, although it might also affect, to a lower extent, the rest of the atoms in the system. This effect is expected since the superstructure modulation $0.21\mathbf{b}_o^*$ does also depend on the different doping level (not shown). Actually, this secondary effect is a constraint for the development of an atomic model accounting for the new observed diffuse features due to the lack of a proper average structure for the samples at different doping levels. In this context, it is worth noting that recent theoretical results motivated by STM investigations[33,34] also directly relates the electronic properties of BISCO compounds with atomic displacements, namely Bi, induced by the interstitial oxygens; what this work does however not take into account is that such displacements can order on a short range as reported here. Furthermore, other STM results[31,32] have shown signatures of a doubling periodicity along the $\mathbf{a}_o$ direction, which are however different in nature. In the first case[31] the modulation seems to be uniform over one part of the sampled region and it has been interpreted as a modulation of the CuO$_2$ planes. Though in principle it might be compatible with our observation further experimental data will be necessary to confirm its extent. On the other hand, the STM data from Pan *et al.* also show some doubling along the same orthorhombic direction. However, before drawing a conclusion some additional data would be required.

In any case and even considering that all the observations relate the observed 2DSRO with oxygen doping, the data also indicate that there is a real link between the SRO and the electronic properties in the bismuth family compounds. This relation is manifested through the relation of the 2DSRO with the T_c. Although we cannot give a precise description of the local order itself a global and nonconventional approach consistent with our data could be as follows:

(i) The one and two layers bismuth cuprates are structurally and as a consequence electronically inhomogeneous.

(ii) 2DSRO regions in the Bi-O layers, triggered by ordering of the doping oxygen, might be electronically mirrored by charge order in the conducting Cu-O plane.

(iii) For low doping levels these regions only extend over a few lattice constants and are far from each other. Here no superconductivity is observed.

(iv) With increasing doping these regions grow in size, possibly connect in some cases with each other, and form a loose network and one starts to observe superconductivity.

(v) At optimal doping most of these regions reach a maximum size (about 60 Å), connect and form a relatively dense network and T_c is maximum.

(vi) Beyond optimal doping these regions start overlapping with each other destroying partially the local ordering (too much oxygen), the remaining ordered parts decrease in size, loosening again their network, and T_c decreases.

(vii) For too high doping levels these ordered regions become so small or disappear completely and with them superconductivity.

VII. CONCLUSIONS

In summary, we have presented a detailed investigation of the $2\mathbf{a}_o$ SRO structure recently observed in optimal Bi-2212

superconductors at room temperature. Experiments as a function of the temperature and the doping level have been performed in Bi-2212 compounds and at optimal doping and room temperature in Bi-2201. The results as a function of the temperature have shown the presence of two distinct regimes: in the low temperature range, from the superconducting state up to 450 K, the diffuse structure has a 2D character and exhibits a $2\mathbf{a}_o$ periodicity. While the associated domain size is constant between 35 K and room temperature, it further diminishes and eventually disappears at about 450 K. The temperature behavior of the diffuse intensity does not follow the same trend as previously observed for "stripes" or phonons. Above 450 K, diffuse intensity located in reciprocal planes perpendicular to the tetragonal axis and with a periodicity corresponding to the $\mathbf{a}_t$ unit cell vector develop; it can be unambiguously ascribed to the presence of linear and uncorrelated chains along the tetragonal directions. The provided data do not allow either to establish or to discard the existence of a link between the two diffuse features.

The low temperature SRO has been shown to be present in Bi-2201 and in Bi-2212 compounds with different doping levels. In all cases the SRO structure is commensurate, with doubled periodicity along the $\mathbf{a}_o$ orthorhombic direction, thus being perpendicular to the already reported superstructure modulation. Furthermore, it originates from atomic displacements with 2D character, the domains being parallel to the $\mathbf{a}_o$-$\mathbf{b}_o$ conduction plane. The only difference observed among the different samples is the variation in the integrated intensity and the domain size ascribed to it. At optimal doping, it varies from 60 Å for the Bi-2212 to 48 Å for the Bi-2201 compound. The domain size as a function of doping level has

been shown to be related with T_c, which is also related with the different oxygen doping of the samples, therefore establishing a straightforward connection of the observed diffuse structure with superconductivity in these compounds.

The question that remains is to establish whether the observations reported here are also present in compounds other than the 1 and 2 layered Bi based superconductors, or in a more restricted way at least in others presenting a lattice modulation, but this is left for future investigations.

After this paper was submitted and while it was being revised, Castellan *et al.*[48] confirmed the existence of 2DSRO in optimally doped Bi-2212 samples. Besides and overall agreement in the present data, there are some differences namely in the diffuse intensity, which we find much stronger, and the extent of the local order. This last point may be explained by the use of correlation length versus domain size which alone could account for the observed factor of 2 difference.

[1] L. P. Gorkov and A. V. Sokol, JETP Lett. **46**, 420 (1987).

[2] J. Zaanen and O. Gunnarsson, Phys. Rev. B **40**, 7391 (1989).

[3] V. J. Emery and S. A. Kivelson, Phys. Rev. Lett. **64**, 475 (1990); Physica C **209**, 597 (1993); V. J. Emery, S. A. Kivelson, and J. M. Tranquada, Proc. Natl. Acad. Sci. U.S.A. **96**, 8814 (1999).

[4] S. Barisic, I. Mrkonjic and I. Kupcic, Physica A **10**, 169 (2001).

[5] J. Friedel and M. Kohmoto, Eur. Phys. J. B **30**, 427 (2002).

[6] A. Damascelli, Z.-X Shen, and Z Hussain, Rev. Mod. Phys. **75**, 473 (2003).

[7] T. Timusk and B. Statt, Rep. Prog. Phys. **62**, 61 (1999).

[8] S. A. Kivelson, I. P. Bindloss, E. Frandkin, V. Oganesyan, J. M. Tranquada, A. Kapitulnik, and C. Howald, Rev. Mod. Phys. **75**, 1201 (2003), and references therein.

[9] S. M. Hayden, G. H. Lander, J. Zarestky, P. J. Brown, C. Stassis, P. Metcalf, and J. M. Honig, Phys. Rev. Lett. **68**, 1061 (1992).

[10] J. M. Tranquada, N. Ichikawa, and S. Uchida, Phys. Rev. B **59**, 14712 (1999), and references therein.

[11] K. Yamada, C. H. Lee, K. Kurahashi, J. Wada, S. Wakimoto, S. Ueki, H. Kimura, and Y. Endoh, S. Hosoya, G. Shirane, R. J. Birgeneau, M. Greven, M. A. Kastner, and Y. J. Kim, Phys. Rev. B **57**, 6165 (1998), and references therein.

[12] H. A. Mook, P. Dai, S. M. Hayden, G. Aeppli, T. G. Perring, and F. Dogan, Nature (London) **404**, 729 (2000), and references therein.

[13] G. Blumberg, M. V. Klein, and S.-W. Cheong, Phys. Rev. Lett. **80**, 564 (1998).

[14] T. Suzuki, T. Goto, K. Chiba, T. Shinoda, T. Fukase, H. Kimura, K. Yamada, M. Ohashi, and Y. Yamaguchi, Phys. Rev. B **57**, R3229 (1998).

[15] H. F. Fong, P. Bourges, Y. Sidis, L. P. Regnault, A. Ivanov, G. D. Gu, N. Koshizuka, and B. Keimer, Nature (London) **398**, 588 (1999).

[16] R. J. McQueeney, Y. Petrov, T. Egami, M. Yethiraj, G. Shirane, and Y. Endoh, Phys. Rev. Lett. **82**, 628 (1999).

[17] L. Pintschovius and M. Braden, Phys. Rev. B **60**, R15039 (1999).

[18] H. Yoshizawa, T. Kakeshita, R. Kajimoto, T. Tanabe, T. Katsufuji, and Y. Tokura, Phys. Rev. B **61**, R854 (2000).

[19] V. Hinkov, S. Pailhès, P. Bourges, Y. Sidis, A. Ivanov, A. Kulakov, C. T. Lin, D. P. Chen, C. Berhnard, and B. Kelmer, Nature (London) **430**, 650 (2004).

[20] M. von Zimmermann, A. Vigliante, T. Niemöller, N. Ichikawa, T. Frello, J. Madsen, P. Wochner, S. Uchida, N. H. Andersen, J. M. Tranquada, D. Gibbs, and J. R. Schneider, Europhys. Lett. **41**, 629 (1998).

[21] E. D. Isaacs, G. Aeppli, P. Zschack, S.-W. Cheong, H. Williams, and D. J. Buttrey, Phys. Rev. Lett. **72**, 3421 (1994).

[22] W. Dmowski, R. J. McQueeney, T. Egami, Y. P. Feng, S. K. Sinha, T. Hinatsu, and S. Uchida, Phys. Rev. B **52**, 6829 (1995).

[23] D. de Fontaine, V. Ozolins, Z. Islam, and S. C. Moss, Phys. Rev. B **71**, 212504 (2005).

[24] N. H. Andersen, M. von Zimmermann, T. Frello, M. Käll, D. Mønster, P.-A. Lindgård, J. Madsen, T. Niemöller, H. F. Poulsen, O. Schmidt, J. R. Schneider, Th. Wolf, P. Donsanjh, R. Liang, and W. H. Hardy, Physica C **317-318**, 259 (1999).

[25] J. Strempfer, I. Zegkinoglou, U. Rutt, M. v. Zimmermann, C. Bernhard, C. T. Lin, Th. Wolf, and B. Keimer, Phys. Rev. Lett. **93**, 157007 (2004).

[26] X. Jiang, P. Wochner, S. C. Moss, and P. Zschack, Phys. Rev. Lett. **67**, 2167 (1991) and references therein.

[27] Z.-X. Cai, Y. Zhu, and D. O. Welch, Phys. Rev. B **46**, 11014 (1992).

[28] Z. Islam, S. K. Sinha, D. Haskel, J. C. Lang, G. Srajer, B. W. Veal, D. R. Haeffner, and H. A. Mook, Phys. Rev. B **66**, 092501 (2002).

[29] V. P. Plakhty, Y. P. Chernenkov, V. I. Fedorov, A. B. Stratilatov, G. A. Emelcheko, and V. A. Tatarchenko, Solid State Commun. **73**, 225 (1990).

[30] Z. Islam, X. Liu, S. K. Sinha, J. C. Lang, S. C. Moss, D. Haskel, G. Srajer, P. Wochner, D. R. Lee, D. R. Haeffner, and U. Welp, Phys. Rev. Lett. **93**, 157008 (2004).

[31] S. Sugita, T. Watanabe, and A. Matsuda, Phys. Rev. B **62**, 8715 (2000).

[32] S. H. Pan, J. P. O'Neal, R. L. Badzey, C. Chamon, H. Ding, J. R. Engelbrecht, Z. Wang, H. Eisaki, S. Uchida, A. K. Gupta, K.-W. Ng, E. W. Hudson, K. M. Lang, and J. C. Davis, Nature (London) **413**, 8653 (2001).

[33] T. S. Nunner, B. M. Andersen, A. Melikyan, and P. J. Hirschfeld, Phys. Rev. Lett. **95**, 177003 (2005).

[34] Y. He, T. S. Nunner, P. J. Hirschfeld, and H.-P. Cheng, Phys. Rev. Lett. **96**, 197002 (2006).

[35] S. Megtert, M. Izquierdo, J. Avila, P. A. Albouy, G. Gu, M. C. Asensio, and R. Comes, J. Phys. IV **130**, 333 (2004); M. Izquierdo, Ph.D. thesis, University Autónoma de Madrid.

[36] J. E. Fischer, P. A. Heiney, P. K. Davies, and D. Vaknin, Phys. Rev. B **39**, 2752 (1989).

[37] A. Guinier, *X-Rays Diffraction in Crystals, Imperfect Crystals and Amorphous Bodies* (Dover, New York, 1994).

[38] G. Gu, K. Takamuku, N. Koshizuka, and S. Tanaka, J. Cryst. Growth **130**, 325 (1993).

[39] G. Yang, J. S. Abell, P. Shang, I. P. Jones, and C. E. Gough, J. Cryst. Growth **166**, 820 (1996).

[40] G. Gu (private communication).

[41] J. L. Tallon, C. Bernhard, H. Shaked, R. L. Hitterman, and J. D. Jorgensen, Phys. Rev. B **51**, 12911 (1995).

[42] C. C. Torardi, M. A. Subramanian, J. C. Calabrese, J. Gopalakrishnan, E. M. McCarron, K. J. Morrissey, T. R. Askew, R. B. Flippen, U. Chowdhry, and A. W. Sleight, Phys. Rev. B **38**, 225 (1988).

[43] H. Raffy (private communication).

[44] R. Comes and G. Shirane, Phys. Rev. B **5**, 1886 (1972); B. Borne and R. Comes, in *Dynamics of Solids and Crystals by Neutron Scattering*, edited by S. W. Lovesey and T. Springer (Springer, New York, 1977).

[45] Y. Le Page, W. R. McKinnon, J. M. Tarascon, and P. Barboux, Phys. Rev. B **40**, 6810 (1989).

[46] B. I. Spivak and S. A. Kivelson, Phys. Rev. B **43**, 3740 (1991); **70**, 155114 (2004).

[47] B. Valenzuela, M. A. H Vozmediano, and F. Guinea, Phys. Rev. B **62**, 11312 (2000).

[48] J. P. Castellan, B. D. Gaulin, H. A. Dabkowska, A. Nabialek, G. Gu, X. Liu, and Z. Islam, Phys. Rev. B **73**, 174505 (2006).